

Solar cell efficiency tables (Version 53)

Martin A. Green¹  | Yoshihiro Hishikawa²  | Ewan D. Dunlop³ | Dean H. Levi⁴ |
Jochen Hohl-Ebinger⁵ | Masahiro Yoshita² | Anita W.Y. Ho-Baillie¹ 

¹School of Photovoltaic and Renewable Energy Engineering, Australian Centre for Advanced Photovoltaics, University of New South Wales, Sydney 2052, Australia

²Research Center for Photovoltaics (RCPV), National Institute of Advanced Industrial Science and Technology (AIST), Central 2, Umezono 1-1-1, Tsukuba, Ibaraki 305-8568, Japan

³Directorate C—Energy, Transport and Climate, European Commission—Joint Research Centre, Via E. Fermi 2749, IT-21027, Ispra (VA), Italy

⁴National Renewable Energy Laboratory, 15013 Denver West Parkway, Golden, CO 80401, USA

⁵Department of Characterisation and Simulation/CalLab Cells, Fraunhofer-Institute for Solar Energy Systems, Heidenhofstr. 2, D-79110 Freiburg, Germany

Correspondence

Martin A. Green, School of Photovoltaic and Renewable Energy Engineering, University of New South Wales, Sydney 2052, Australia.
Email: m.green@unsw.edu.au

Abstract

Consolidated tables showing an extensive listing of the highest independently confirmed efficiencies for solar cells and modules are presented. Guidelines for inclusion of results into these tables are outlined and new entries since July 2018 are reviewed.

KEYWORDS

energy conversion efficiency, photovoltaic efficiency, solar cell efficiency

1 | INTRODUCTION

Since January 1993, “*Progress in Photovoltaics*” has published six monthly listings of the highest confirmed efficiencies for a range of photovoltaic cell and module technologies.^{1–3} By providing guidelines for inclusion of results into these tables, this not only provides an authoritative summary of the current state-of-the-art but also encourages researchers to seek independent confirmation of results and to report results on a standardised basis. In Version 33 of these tables,³ results were updated to the new internationally accepted reference spectrum (International Electrotechnical Commission IEC 60904-3, Ed. 2, 2008).

The most important criterion for inclusion of results into the tables is that they must have been independently measured by a recognised test centre listed elsewhere.² A distinction is made between three different eligible definitions of cell area: total area, aperture area, and designated illumination area, as also defined elsewhere² (note that, if masking is used, masks must have a simple aperture geometry, such as square, rectangular, or circular). “Active area” efficiencies are not included. There are also certain minimum

values of the area sought for the different device types (above 0.05 cm² for a concentrator cell, 1 cm² for a one-sun cell, 800 cm² for a module and 200 cm² for a “submodule”).

Results are reported for cells and modules made from different semiconductors and for sub-categories within each semiconductor grouping (eg. crystalline, polycrystalline, and thin film). From Version 36 onwards, spectral response information is included (when possible) in the form of a plot of the external quantum efficiency (EQE) versus wavelength, either as absolute values or normalised to the peak measured value. Current-voltage (IV) curves have also been included where possible from Version 38 onwards. A graphical summary of progress over the first 25 years during which the tables have been published has been included in Version 51.²

Highest confirmed “one sun” cell and module results are reported in Tables 1–4. Any changes in the tables from those previously published¹ are set in bold type. In most cases, a literature reference is provided that describes either the result reported, or a similar result (readers identifying improved references are welcome to submit to the lead author). Table 1 summarizes the best-reported measurements for “one-sun” (non-concentrator) single-junction cells and submodules.

TABLE 1 Confirmed single-junction terrestrial cell and submodule efficiencies measured under the global AM1.5 spectrum (1000 W/m²) at 25°C (IEC 60904-3: 2008, ASTM G-173-03 global)

Classification	Efficiency, %	Area, cm ²	V _{oc} , V	J _{sc} , mA/cm ²	Fill Factor, %	Test Centre (date)	Description
<u>Silicon</u>							
Si (crystalline cell)	26.7 ± 0.5	79.0 (da)	0.738	42.65 ^a	84.9	AIST (3/17)	Kaneka, n-type rear IBC ⁴
Si (multicrystalline cell)	22.3 ± 0.4 ^b	3.923 (ap)	0.6742	41.08 ^c	80.5	FhG-ISE (8/17)	FhG-ISE, n-type ⁵
Si (thin transfer submodule)	21.2 ± 0.4	239.7 (ap)	0.687 ^d	38.50 ^{d,e}	80.3	NREL (4/14)	Solexel (35 µm thick) ⁶
Si (thin film minimodule)	10.5 ± 0.3	94.0 (ap)	0.492 ^d	29.7 ^{d,f}	72.1	FhG-ISE (8/07)	CSG Solar (<2 µm on glass) ⁷
<u>III-V cells</u>							
GaAs (thin film cell)	29.1 ± 0.6	0.998 (ap)	1.1272	29.78 ^g	86.7	FhG-ISE (10/18)	Alta Devices ⁸
GaAs (multicrystalline)	18.4 ± 0.5	4.011 (t)	0.994	23.2	79.7	NREL (11/95)	RTI, Ge substrate ⁹
InP (crystalline cell)	24.2 ± 0.5 ^b	1.008 (ap)	0.939	31.15 ^a	82.6	NREL (3/13)	NREL ¹⁰
<u>Thin film chalcogenide</u>							
CIGS (cell)	22.9 ± 0.5	1.041 (da)	0.744	38.77 ^h	79.5	AIST (11/17)	Solar Frontier ^{11,12}
CdTe (cell)	21.0 ± 0.4	1.0623 (ap)	0.8759	30.25 ^e	79.4	Newport (8/14)	First Solar, on glass ¹³
CZTSSe (cell)	11.3 ± 0.3	1.1761 (da)	0.5333	33.57 ^g	63.0	Newport (10/18)	DGIST, Korea ¹⁴
CZTS (cell)	10.0 ± 0.2	1.113 (da)	0.7083	21.77 ^a	65.1	NREL (3/17)	UNSW ¹⁵
<u>Amorphous/microcrystalline</u>							
Si (amorphous cell)	10.2 ± 0.3 ^{ib}	1.001 (da)	0.896	16.36 ^e	69.8	AIST (7/14)	AIST ¹⁶
Si (microcrystalline cell)	11.9 ± 0.3 ^b	1.044 (da)	0.550	29.72 ^a	75.0	AIST (2/17)	AIST ¹⁶
<u>Perovskite</u>							
Perovskite (cell)	20.9 ± 0.7 ^{ij}	0.991 (da)	1.125	24.92 ^c	74.5	Newport (7/17)	KRICT ¹⁷
Perovskite (minimodule)	17.25 ± 0.6 ^{ij}	17.277 (da)	1.070 ^d	20.66 ^{d,h}	78.1	Newport (5/18)	Microquanta, 7 serial cells ¹⁸
Perovskite (submodule)	11.7 ± 0.4 ⁱ	703 (da)	1.073 ^d	14.36 ^{d,h}	75.8	AIST (3/18)	Toshiba, 44 serial cells ¹⁹
<u>Dye sensitised</u>							
Dye (cell)	11.9 ± 0.4 ^{ik}	1.005 (da)	0.744	22.47 ⁿ	71.2	AIST (9/12)	Sharp ²⁰
Dye (minimodule)	10.7 ± 0.4 ^{il}	26.55 (da)	0.754 ^d	20.19 ^{d,o}	69.9	AIST (2/15)	Sharp, 7 serial cells ²¹
Dye (submodule)	8.8 ± 0.3 ⁱ	398.8 (da)	0.697 ^d	18.42 ^{d,p}	68.7	AIST (9/12)	Sharp, 26 serial cells ²²
<u>Organic</u>							
Organic (cell)	11.2 ± 0.3 ^q	0.992 (da)	0.780	19.30 ^e	74.2	AIST (10/15)	Toshiba ²³
Organic (minimodule)	9.7 ± 0.3 ^q	26.14 (da)	0.806 ^d	16.47 ^{d,o}	73.2	AIST (2/15)	Toshiba (8 series cells) ²³

Abbreviations: AIST, Japanese National Institute of Advanced Industrial Science and Technology; (ap), aperture area; a-Si, amorphous silicon/hydrogen alloy; CIGS, CuIn_{1-y}Ga_ySe₂; CZTS, Cu₂ZnSnS₄; CZTSSe, Cu₂ZnSnS_{4-y}Se_y; (da), designated illumination area; FhG-ISE, Fraunhofer Institut für Solare Energiesysteme; nc-Si, nanocrystalline or microcrystalline silicon; (t), total area.

^aSpectral response and current-voltage curve reported in Version 50 of these tables.

^bNot measured at an external laboratory.

^cSpectral response and current-voltage curve reported in Version 51 of these tables.

^dReported on a "per cell" basis.

^eSpectral responses and current-voltage curve reported in Version 45 of these tables.

^fRecalibrated from original measurement.

^gSpectral response and current-voltage curve reported in the present version of these tables.

^hSpectral response and current-voltage curve reported in Version 52 of these tables.

ⁱStabilized by 1000-h exposure to 1 sun light at 50 °C.

^jInitial performance. References 67 and 68 review the stability of similar devices.

^kAverage of forward and reverse sweeps at 150 mV/s (hysteresis ± 0.26%).

^lMeasured using 13 point IV sweep with constant bias until data constant at 0.05% level.

^mInitial efficiency. Reference 71 reviews the stability of similar devices.

ⁿSpectral response and current-voltage curve reported in Version 41 of these tables.

^oSpectral response and current-voltage curve reported in Version 46 of these tables.

^pSpectral response and current-voltage curve reported in Version 43 of these tables.

^qInitial performance. References 69 and 70 review the stability of similar devices.

TABLE 2 “Notable exceptions” for single-junction cells and submodules: “Top dozen” confirmed results, not class records, measured under the global AM1.5 spectrum (1000 W m^{-2}) at 25°C (IEC 60904-3:2008, ASTM G-173-03 global)

Classification	Efficiency, %	Area, cm^2	V_{oc} , V	J_{sc} , mA/cm^2	Fill Factor, %	Test Centre (Date)	Description
Cells (silicon)							
Si (crystalline)	25.0 ± 0.5	4.00 (da)	0.706	42.7^a	82.8	Sandia (3/99) ^b	UNSW p-type PERC top/rear contacts ²⁴
Si (crystalline)	25.8 ± 0.5^c	4.008 (da)	0.7241	42.87^d	83.1	FhG-ISE (7/17)	FhG-ISE, n-type top/rear contacts ²⁵
Si (crystalline)	26.1 ± 0.3^e	3.9857 (da)	0.7266	42.62^e	84.3	ISFH (2/18)	ISFH, p-type rear IBC ²⁶
Si (large)	26.6 ± 0.5	179.74 (da)	0.7403	42.5^f	84.7	FhG-ISE (11/16)	Kaneka, n-type rear IBC ⁴
Si (multicrystalline)	22.0 ± 0.4	245.83 (t)	0.6717	40.55^d	80.9	FhG-ISE (9/17)	Jinko solar, large p-type ²⁷
Cells (III-V)							
GaInP	21.4 ± 0.3	0.2504 (ap)	1.4932	16.31^g	87.7	NREL (9/16)	LG electronics, high bandgap ²⁸
GaInAsP/GaInAs	32.6 ± 1.4^c	0.248 (ap)	2.024	19.51^d	82.5	NREL (10/17)	NREL, monolithic tandem ²⁹
Cells (chalcogenide)							
CdTe (thin-film)	22.1 ± 0.5	0.4798 (da)	0.8872	31.69^h	78.5	Newport (11/15)	First solar on glass ³⁰
CZTSSe (thin-film)	12.6 ± 0.3	0.4209 (ap)	0.5134	35.21^i	69.8	Newport (7/13)	IBM solution grown ³¹
CZTSSe (thin-film)	12.6 ± 0.3	0.4804 (da)	0.5411	35.39	65.9	Newport (10/18)	DGIST, Korea ¹⁴
CZTS (thin-film)	11.0 ± 0.2	0.2339 (da)	0.7306	21.74^f	69.3	NREL (3/17)	UNSW on glass ³²
Cells (other)							
Perovskite (thin-film)	$23.7 \pm 0.8^{j,k}$	0.0739 (ap)	1.1697	25.40 ^l	79.8	Newport (9/18)	ISCAS, Beijing ³³
Organic (thin-film)	15.6 ± 0.2^m	0.4113 (da)	0.8381	25.03 ^l	74.5	NREL (11/18)	5th China U. - Central 5th U. ³⁴

Abbreviations: AIST, Japanese National Institute of Advanced Industrial Science and Technology; (ap), aperture area; CIGSSe, CuInGaSSe; CZTS, $\text{Cu}_2\text{ZnSnS}_4$; CZTSSe, $\text{Cu}_2\text{ZnSnS}_{4-x}\text{Se}_x$; (da), designated illumination area; FhG-ISE, Fraunhofer-Institut für Solare Energiesysteme; ISFH, Institute for Solar Energy Research, Hamelin; NREL, National Renewable Energy Laboratory; (t), total area.

^aSpectral response reported in Version 36 of these tables.

^bRecalibrated from original measurement.

^cNot measured at an external laboratory.

^dSpectral response and current-voltage curves reported in Version 51 of these tables.

^eSpectral response and current-voltage curve reported in Version 52 of these tables.

^fSpectral response and current-voltage curves reported in Version 50 of these tables.

^gSpectral response and current-voltage curves reported in Version 49 of these tables.

^hSpectral response and/or current-voltage curves reported in Version 46 of these tables.

ⁱSpectral response and current-voltage curves reported in Version 44 of these tables.

^jStability not investigated. References 67 and 68 document stability of similar devices.

^kMeasured using 13-point IV sweep with constant voltage bias until current determined as unchanging.

^lSpectral response and current-voltage curve reported in the present version of these tables.

^mLong-term stability not investigated. References 69 and 70 document stability of similar devices.

TABLE 3 Confirmed multiple-junction terrestrial cell and submodule efficiencies measured under the global AM1.5 spectrum (1000 W/m²) at 25°C (IEC 60904-3: 2008, ASTM G-173-03 global)

Classification	Efficiency, %	Area, cm ²	Voc, V	Jsc, mA/cm ²	Fill Factor, %	Test Centre (Date)	Description
III-V multijunctions							
5 junction cell (bonded)	38.8 ± 1.2	1.021 (ap)	4.767	9.564	85.2	NREL (7/13)	Spectrolab, 2-terminal ³⁵
(2.17/1.68/1.40/1.06/0.73 eV)							
InGaP/GaAs/InGaAs	37.9 ± 1.2	1.047 (ap)	3.065	14.27 ^a	86.7	AIST (2/13)	Sharp, 2 term. ³⁶
GaInP/GaAs (monolithic)	32.8 ± 1.4	1.000 (ap)	2.568	14.56 ^b	87.7	NREL (9/17)	LG electronics, 2 term.
Multijunctions with c-Si							
GaInP/GaAs/Si (mech. stack)	35.9 ± 0.5 ^c	1.002 (da)	2.52/0.681	13.6/11.0	87.5/78.5	NREL (2/17)	NREL/CSEM/EPFL, 4-term. ³⁷
GaInP/GaAs/Si (wafer bonded)	33.3 ± 1.2 ^c	3.984 (ap)	3.127 ^b	12.7 ^b	83.5	FhG-ISE (8/17)	Fraunhofer ISE, 2-term. ³⁸
GaInP/GaAs/Si (monolithic)	22.3 ± 0.8 ^c	0.994 (ap)	2.619	10.0 ^d	85.0	FhG-ISE (10/18)	Fraunhofer ISE, 2-term. ³⁹
GaAsP/Si (monolithic)	20.1 ± 1.3	3.940 (ap)	1.673	14.94 ^e	80.3	NREL (5/18)	OSU/SolAero/UNSW, 2-term.
GaAs/Si (mech. Stack)	32.8 ± 0.5 ^c	1.003 (da)	1.09/0.683	28.9/11.1 ^e	85.0/79.2	NREL (12/16)	NREL/CSEM/EPFL, 4-term. ³⁷
Perovskite/Si (monolithic)	27.3 ± 0.8 ^f	1.090 (da)	1.813	19.99 ^d	75.4	FhG-ISE (6/18)	Oxford PV ⁴⁰
GaInP/GaInAs/Ge, Si (spectral split minimodule)	34.5 ± 2.0	27.83 (ap)	2.66/0.65	13.1/9.3	85.6/79.0	NREL (4/16)	UNSW/Azur/Trina, 4-term. ⁴¹
a-Si/nc-Si multijunctions							
a-Si/nc-Si/nc-Si (thin-film)	14.0 ± 0.4 ^{g,c}	1.045 (da)	1.922	9.94 ^h	73.4	AIST (5/16)	AIST, 2-term. ⁴²
a-Si/nc-Si (thin-film cell)	12.7 ± 0.4 ^{g,c}	1.000 (da)	1.342	13.45 ⁱ	70.2	AIST (10/14)	AIST, 2-term. ¹⁶
Notable exception							
Perovskite/CIGS ^j	22.4 ± 1.9 ^f	0.042 (da)	1.774	17.3 ^g	73.1	NREL (11/17)	UCLA, 2-term. ⁴³
GaInP/GaAs/GaInAs	37.8 ± 1.4	0.998 (ap)	3.013	14.60 ^d	85.8	NREL (1/18)	Microlink (ELO) ⁴⁴

Abbreviations: AIST, Japanese National Institute of Advanced Industrial Science and Technology; (ap), aperture area; a-Si, amorphous silicon/hydrogen alloy; (da), designated illumination area; FhG-ISE, Fraunhofer Institut für Solare Energiesysteme; nc-Si, nanocrystalline or microcrystalline silicon; (t), total area.

^aSpectral response and current-voltage curve reported in Version 42 of these tables.

^bSpectral response and current-voltage curve reported in the Version 51 of these tables.

^cNot measured at an external laboratory.

^dSpectral response and current-voltage curve reported in the present version of these tables.

^eSpectral response and current-voltage curve reported in Version 50 or 52 of these tables.

^fInitial efficiency. References 67 and 68 review the stability of similar perovskite-based devices.

^gStabilized by 1000-h exposure to 1 sun light at 50 °C.

^hSpectral response and current-voltage curve reported in Version 49 of these tables.

ⁱSpectral responses and current-voltage curve reported in Version 45 of these tables.

^jArea too small to qualify as outright class record.

TABLE 4 Confirmed terrestrial module efficiencies measured under the global AM1.5 spectrum (1000 W/m²) at a cell temperature of 25°C (IEC 60904-3: 2008, ASTM G-173-03 global)

Classification	Effic., %	Area, cm ²	V _{oc} , V	I _{sc} , A	FF, %	Test Centre (Date)	Description
Si (crystalline)	24.4 ± 0.5	13177 (da)	79.5	5.04 ^a	80.1	AIST (9/16)	Kaneka (108 cells) ⁴
Si (multicrystalline)	19.9 ± 0.4	15143 (ap)	78.87	4.795 ^a	79.5	FhG-ISE (10/16)	Trina solar (120 cells) ⁴⁵
GaAs (thin film)	25.1 ± 0.8	866.45 (ap)	11.08	2.303 ^b	85.3	NREL (11/17)	Alta devices ⁴⁶
CIGS (Cd free)	19.2 ± 0.5	841 (ap)	48.0	0.456 ^b	73.7	AIST (1/17)	Solar frontier (70 cells) ⁴⁷
CdTe (thin-film)	18.6 ± 0.5	7038.8 (da)	110.6	1.533 ^d	74.2	NREL (4/15)	First solar, monolithic ⁴⁸
a-Si/nc-Si (tandem)	12.3 ± 0.3 ^f	14322 (t)	280.1	0.902 ^f	69.9	ESTI (9/14)	TEL solar, Trubbach labs ⁴⁹
Perovskite	11.6 ± 0.4 ^g	802 (da)	23.79	0.577 ^h	68.0	AIST (4/18)	Toshiba (22 cells) ¹⁹
Organic	8.7 ± 0.3 ^g	802 (da)	17.47	0.569 ^d	70.4	AIST (5/14)	Toshiba ²³
Multijunction							
InGaP/GaAs/InGaAs	31.2 ± 1.2	968 (da)	23.95	1.506	83.6	AIST (2/16)	Sharp (32 cells) ⁵⁰
Notable exception							
CIGS (large)	15.7 ± 0.5	9703 (ap)	28.24	7.254 ⁱ	72.5	NREL (11/10)	Miasole ⁵¹

Abbreviations: (ap), aperture area; a-Si, amorphous silicon/hydrogen alloy; a-SiGe, amorphous silicon/germanium/hydrogen alloy; CIGSS, CuInGaSSe; (da), designated illumination area; Effic., efficiency; FF, fill factor; nc-Si, nanocrystalline or microcrystalline silicon; (t), total area.

^aSpectral response and current voltage curve reported in Version 49 of these tables.

^bSpectral response and current-voltage curve reported in Version 50 or 51 of these tables.

^cSpectral response and/or current-voltage curve reported in Version 47 of these tables.

^dSpectral response and current-voltage curve reported in Version 45 of these tables.

^eStabilised at the manufacturer to the 2% level following IEC procedure of repeated measurements.

^fSpectral response and/or current-voltage curve reported in Version 46 of these tables.

^gInitial performance. References 67 and 70 review the stability of similar devices.

^hSpectral response and current-voltage curve reported in the present version of these tables.

ⁱSpectral response reported in Version 37 of these tables.

TABLE 5 Terrestrial concentrator cell and module efficiencies measured under the ASTM G-173-03 direct beam AM1.5 spectrum at a cell temperature of 25°C

Classification	Effic., %	Area, cm ²	Intensity ^a , suns	Test Centre (Date)	Description
<u>Single cells</u>					
GaAs	30.5 ± 1.0 ^b	0.10043 (da)	258	NREL (10/18)	NREL, 1-junction
Si	27.6 ± 1.2 ^c	1.00 (da)	92	FhG-ISE (11/04)	Amonix back-contact ⁵²
CIGS (thin-film)	23.3 ± 1.2 ^{d,e}	0.09902 (ap)	15	NREL (3/14)	NREL ⁵³
<u>Multijunction cells</u>					
GaInP/GaAs, GaInAsP/GaInAs	46.0 ± 2.2 ^f	0.0520 (da)	508	AIST (10/14)	Soitec/CEA/FhG-ISE 4j bonded ⁵⁴
GaInP/GaAs/GaInAs/GaInAs	45.7 ± 2.3 ^{d,g}	0.09709 (da)	234	NREL (9/14)	NREL, 4j monolithic ⁵⁵
InGaP/GaAs/InGaAs	44.4 ± 2.6 ^h	0.1652 (da)	302	FhG-ISE (4/13)	Sharp, 3j inverted metamorphic ⁵⁶
GaInAsP/GaInAs	35.5 ± 1.2 ^{i,d}	0.10031 (da)	38	NREL (10/17)	NREL 2-junction (2j)
<u>Minimodule</u>					
GaInP/GaAs, GaInAsP/GaInAs	43.4 ± 2.4 ^{d,j}	18.2 (ap)	340 ^k	FhG-ISE (7/15)	Fraunhofer ISE 4j (lens/cell) ⁵⁷
<u>Submodule</u>					
GaInP/GaInAs/Ge, Si	40.6 ± 2.0 ^j	287 (ap)	365	NREL (4/16)	UNSW 4j split spectrum ⁵⁸
<u>Modules</u>					
Si	20.5 ± 0.8 ^d	1875 (ap)	79	Sandia (4/89) ^l	Sandia/UNSW/ENTECH (12 cells) ⁵⁹
Three junction (3j)	35.9 ± 1.8 ^m	1092 (ap)	N/A	NREL (8/13)	Amonix ⁶⁰
Four junction (4j)	38.9 ± 2.5 ⁿ	812.3 (ap)	333	FhG-ISE (4/15)	Soitec ⁶¹
<u>"Notable exceptions"</u>					
Si (large area)	21.7 ± 0.7	20.0 (da)	11	Sandia (9/90) ^k	UNSW laser grooved ⁶²
Luminescent minimodule	7.1 ± 0.2	25(ap)	2.5 ^k	ESTI (9/08)	ECN Petten, GaAs cells ⁶³
4j minimodule	41.4 ± 2.6^d	121.8 (ap)	230	FhG-ISE (9/18)	FhG-ISE, 10 cells⁵⁷

Abbreviations: (ap), aperture area; CIGS, CuInGaSe₂; (da), designated illumination area; Effic., efficiency; FhG-ISE, Fraunhofer-Institut für Solare Energiesysteme; NREL, National Renewable Energy Laboratory.

^aOne sun corresponds to direct irradiance of 1000 Wm⁻².

^bSpectral response and current-voltage curve reported in the present version of these tables.

^cMeasured under a low aerosol optical depth spectrum similar to ASTM G-173-03 direct⁷².

^dNot measured at an external laboratory.

^eSpectral response and current-voltage curve reported in Version 44 of these tables.

^fSpectral response and current-voltage curve reported in Version 45 of these tables.

^gSpectral response and current-voltage curve reported in Version 46 of these tables.

^hSpectral response and current-voltage curve reported in Version 42 of these tables.

ⁱSpectral response and current-voltage curve reported in Version 51 of these tables.

^jDetermined at IEC 62670-1 CSTC reference conditions.

^kGeometric concentration.

^lRecalibrated from original measurement.

^mReferenced to 1000 W/m² direct irradiance and 25°C cell temperature using the prevailing solar spectrum and an in-house procedure for temperature translation.

ⁿMeasured under IEC 62670-1 reference conditions following the current IEC power rating draft 62670-3.

Table 2 contains what might be described as "notable exceptions" for "one-sun" single-junction cells and submodules in the above category. While not conforming to the requirements to be recognized as a class record, the devices in Table 2 have notable characteristics that will be of interest to sections of the photovoltaic community, with entries based on their significance and timeliness. To encourage discrimination, the table is limited to nominally 12 entries with the present authors having voted for their preferences for inclusion. Readers who have suggestions of notable exceptions for inclusion into this or subsequent tables are welcome to contact any of the authors with full details. Suggestions conforming to the guidelines will be included on the voting list for a future issue.

Table 3 was first introduced in Version 49 of these tables and summarizes the growing number of cell and submodule results involving high efficiency, one-sun multiple-junction devices (previously reported in Table 1). Table 4 shows the best results for one-sun modules, both single and multiple junction, while Table 5 shows the best results for concentrator cells and concentrator modules. A small number of "notable exceptions" are also included in Tables 3–5.

2 | NEW RESULTS

Ten new results are reported in the present version of these tables. The first new result in Table 1 (one-sun cells) represents an outright

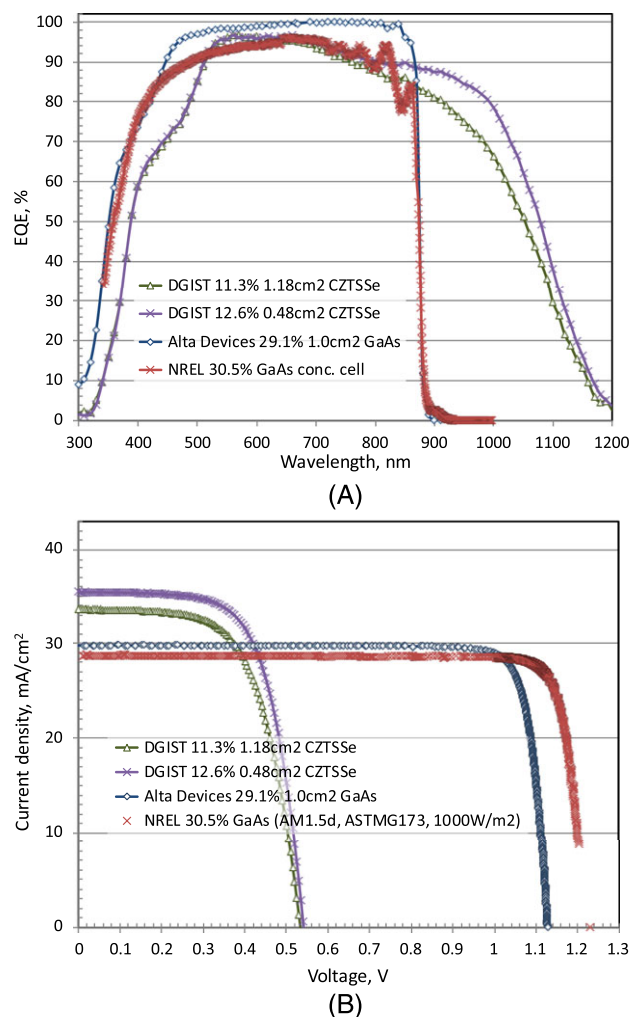


FIGURE 1 A, External quantum efficiency (EQE) for the new GaAs and CZTSSe cell results reported in this issue; B, corresponding current density-voltage (JV) curves for the same devices [Colour figure can be viewed at wileyonlinelibrary.com]

record for any single-junction solar cell. An efficiency of 29.1% was measured for a 1-cm² GaAs cell fabricated by Alta Devices⁸ and measured at the Fraunhofer Institute for Solar Energy Systems (FhG-ISE).

The second new result is an efficiency of 11.3% measured for a 1.2-cm² CZTSSe (Cu₂ZnSnS_xSe_{4-x}) solar cell fabricated by Daegu Gyeongbuk Institute of Science and Technology (DGIST), Korea¹⁴ and measured by the Newport PV Laboratory.

The first of three new results in Table 2 (one-sun “notable exceptions”) equals the previous record for a small area CZTSSe cell. An efficiency of 12.6% was measured also at Newport for a 0.48-cm² cell again fabricated by DGIST. Cell area is too small for classification as an outright record, with solar cell efficiency targets in governmental research programs generally specified in terms of a cell area of 1-cm² or larger.⁶⁴⁻⁶⁶

The second new result in Table 2 represents a new record for a Pb-halide perovskite solar cell, with an efficiency of 23.7% confirmed for a small area 0.07-cm² cell fabricated by the Institute for Semiconductors of the Chinese Academy of Sciences (ISCAS), Beijing³³ and measured at Newport.

For perovskite cells, the tables now accept results based on “quasi-steady-state” measurements (sometimes called “stabilised” in

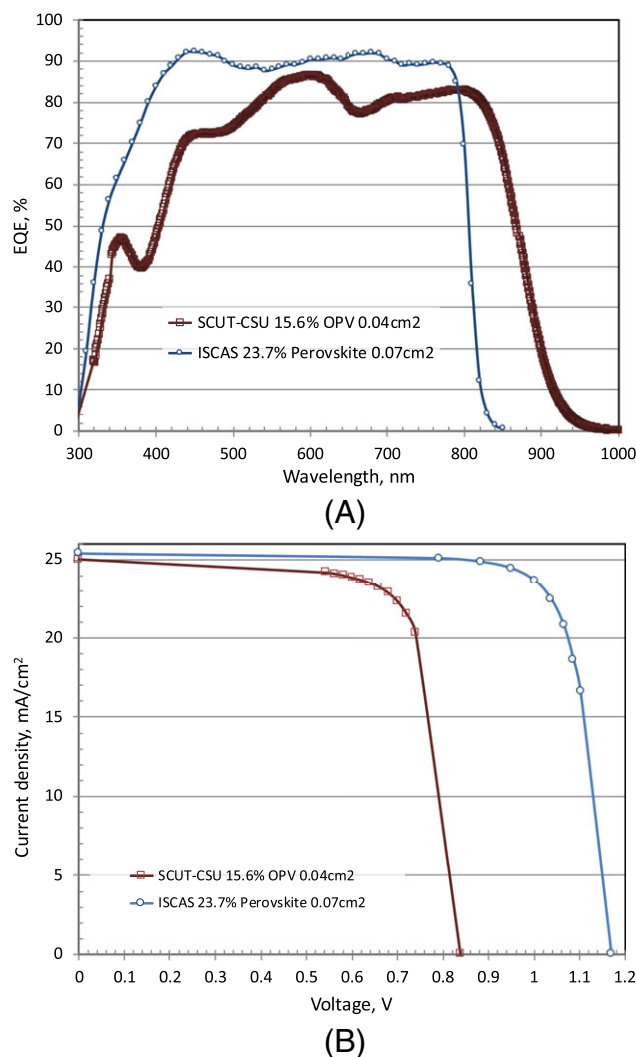


FIGURE 2 A, External quantum efficiency (EQE) for the new OPV and perovskite cell results reported in this issue; B, corresponding current density-voltage (JV) curves [Colour figure can be viewed at wileyonlinelibrary.com]

the perovskite field, although this conflicts with usage in other areas of photovoltaics). Along with other emerging technologies, perovskite cells may not demonstrate the same level of stability as conventional cells, with the stability of perovskite cells discussed elsewhere.^{67,68}

A third new “notable exception” in Table 2 is 13.3% for a very small area 0.04-cm² organic solar cell fabricated by South China University and Central South University³⁴ and measured at the National Renewable Energy Laboratory (NREL). The stability of organic solar cells is discussed elsewhere^{69,70} with cell area again too small for classification as an outright record.

Three new results are reported in Table 3 relating to one-sun, multijunction devices. The first is 23.3% for a 1-cm² monolithic, three-junction, two-terminal GaInP/GaAs/Si tandem device (monolithic, metamorphic, direct growth) fabricated and measured by the Fraunhofer Institute for Solar Energy Systems.³⁹

The second new result reports the demonstration of an efficiency of 27.3% for a 1-cm² perovskite/silicon monolithic two-junction, two-terminal device fabricated by Oxford PV⁴⁰ and again measured by Fraunhofer Institute for Solar Energy System. Note that this efficiency

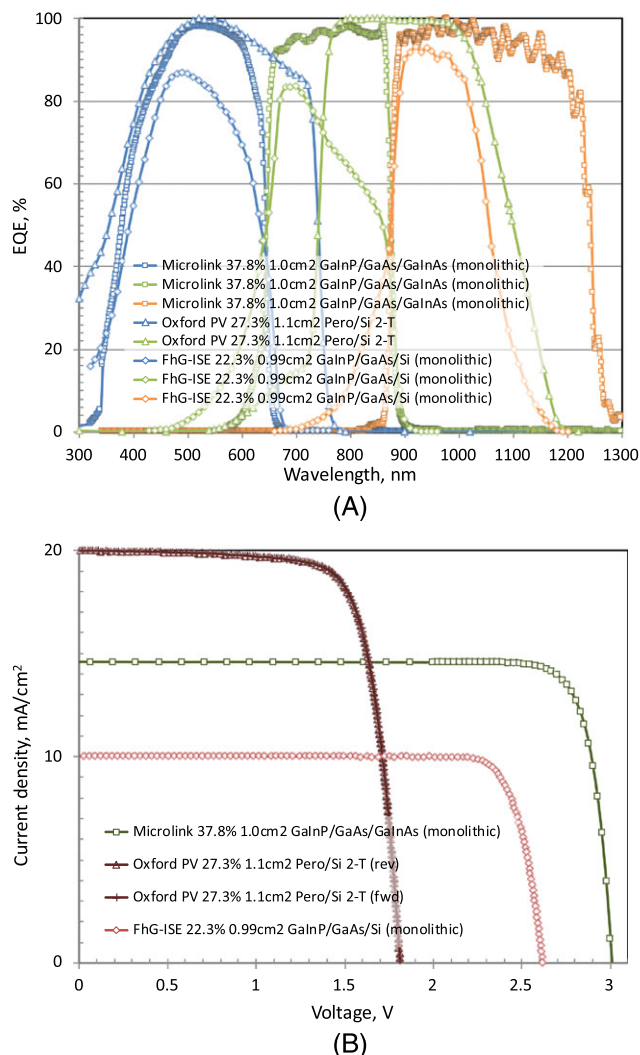


FIGURE 3 A, External quantum efficiency (EQE) for the new multijunction cell results reported in this issue (some results normalised); B, corresponding current density-voltage (JV) curves [Colour figure can be viewed at wileyonlinelibrary.com]

now exceeds the highest efficiency for a single-junction silicon cell (Table 1), although for a much smaller area device.

A third new result for Table 3 is included as a multijunction cell “notable exception.” An efficiency of 37.8% was measured for a 1-cm² GaInP/GaAs/GaInAs monolithic three-junction, two-terminal cell fabricated by Microlink Devices⁴⁴ and measured at NREL. The notable feature of this device is that it was fabricated using epitaxial lift-off from a substrate that can be reused.⁴⁴

Two new results appears in Table 5 (“concentrator cells and modules”). The first is 30.5% efficiency for a single junction GaAs concentrator cell fabricated and measured by NREL.

The second is a “notable exception.” An efficiency of 41.4% is reported for a 122-cm² concentrator minimodule consisting of 10 glass acromatic lenses and 10 wafer-bonded GaInP/GaAs, GaInAsP/GaInAs 4-junction solar cells fabricated and measured by FhG-ISE. This is the highest efficiency measured for such an interconnected concentrator module.

The EQE spectra for the new GaAs and CZTSSe cell results reported in the present issue of these tables are shown in Figure 1A,

with Figure 1B showing the current density-voltage (JV) curves for the same devices. Figure 2A shows the EQE for the new OPV cell and perovskite module results with Figure 2B showing their current JV curves. Figure 3A,B shows the corresponding EQE and JV curves for the new two-junction, two-terminal cell results.

DISCLAIMER

While the information provided in the tables is provided in good faith, the authors, editors, and publishers cannot accept direct responsibility for any errors or omissions.

ACKNOWLEDGEMENT

The Australian Centre for Advanced Photovoltaics commenced operation in February 2013 with support from the Australian Government through the Australian Renewable Energy Agency (ARENA). The Australian Government does not accept responsibility for the views, information, or advice expressed herein. The work by D. Levi was supported by the US Department of Energy under Contract No. DE-AC36-08-GO28308 with the National Renewable Energy Laboratory. The work at AIST was supported in part by the Japanese New Energy and Industrial Technology Development Organisation (NEDO) under the Ministry of Economy, Trade, and Industry (METI).

ORCID

Martin A. Green <https://orcid.org/0000-0002-8860-396X>
Yoshihiro Hishikawa <https://orcid.org/0000-0002-8420-9260>
Anita W.Y. Ho-Baillie <https://orcid.org/0000-0001-9849-4755>

REFERENCES

- Green MA, Emery K, Hishikawa Y, et al. Solar cell efficiency tables (version 52). *Prog Photovolt Res Appl*. 2018;26(7):427-436.
- Green MA, Emery K, Hishikawa Y, et al. Solar cell efficiency tables (version 51). *Prog Photovolt Res Appl*. 2018;26(1):3-12.
- Green MA, Emery K, Hishikawa Y, Warta W. Solar cell efficiency tables (version 33). *Prog Photovolt Res Appl*. 2009;17(1):85-94.
- Yoshikawa K, Kawasaki H, Yoshida W, et al. Silicon heterojunction solar cell with interdigitated back contacts for a photoconversion efficiency over 26%. *Nature Energy*. 2017;2(5):17032.
- Benick J, Richter A, Müller R, et al. High-efficiency n-type HP mc silicon solar cells. *IEEE J Photovoltaics*. 2017;7(5):1171-1175.
- Moslehi MM, Kapur P, Kramer J, et al. World-record 20.6% efficiency 156 mm x 156 mm full-square solar cells using low-cost kerfless ultra-thin epitaxial silicon & porous silicon lift-off technology for industry-leading high-performance smart PV modules. PV Asia Pacific Conference (APVIA/PVAP), 24 October 2012.
- Keevers MJ, Young TL, Schubert U, Green MA. 10% efficient CSG minimodules. 22nd European Photovoltaic Solar Energy Conference, Milan, September 2007.
- Kayes BM, Nie H, Twist R, et al. 27.6% conversion efficiency, a new record for single-junction solar cells under 1 sun illumination. *Proceedings of the 37th IEEE Photovoltaic Specialists Conference*, 2011.
- Venkatasubramanian R, O'Quinn BC, Hills JS, et al. 18.2% (AM1.5) efficient GaAs solar cell on optical-grade polycrystalline Ge substrate. *Conference Record, 25th IEEE Photovoltaic Specialists Conference*, Washington, May 1997, 31-36.
- Wanlass M. Systems and methods for advanced ultra-high-performance InP solar cells. US Patent 9,590,131 B2, 7 March 2017.

11. Solar Frontier Press Release dated 20 December 2017, "Solar frontier achieves world record thin-film solar cell efficiency of 22.9%" (http://www.solar-frontier.com/eng/news/2017/1220_press.html, accessed 9 May 2018).
12. Wu JL, Hirai Y, Kato T, Sugimoto H, Bermudez V. New world record efficiency up to 22.9% for Cu (In,Ga)(Se,S)₂ thin-film solar cells. *7th World Conference on Photovoltaic Energy Conversion (WCPEC-7)*, June 10–15, 2018, Waikoloa, HI, USA.
13. First Solar Press Release, First Solar builds the highest efficiency thin film PV cell on record, 5 August 2014.
14. https://en.dgist.ac.kr/site/dgist_eng/menu/984.do (Accessed October 28, 2018).
15. Yan C, Huang J, Sun K, et al. Cu₂ZnSn S₄ solar cells with over 10% power conversion efficiency enabled by heterojunction heat treatment. *Nature Energy*. 2018;3(9):764–772.
16. Matsui T, Maejima K, Bidiville A, et al. High-efficiency thin-film silicon solar cells realized by integrating stable a-Si:H absorbers into improved device design. *Jpn J Appl Phys*. 2015;54(8S1):08KB10. <https://doi.org/10.7567/JJAP.54.08KB10>
17. Yang WS, Noh JH, Jeon NJ, et al. High-performance photovoltaic perovskite layers fabricated through intramolecular exchange. *Science*. 2015;348(6240):1234–1237.
18. <http://www.microquanta.com> (Accessed 9 May 9, 2018).
19. Toshiba news release dated 25 September 2017 (https://www.toshiba.co.jp/rdc/rd/detail_e/e1709_02.html)
20. Komiya R, Fukui A, Murofushi N, Koide N, Yamanaka R, Katayama H. Improvement of the conversion efficiency of a monolithic type dye-sensitized solar cell module. *Technical Digest, 21st International Photovoltaic Science and Engineering Conference*, Fukuoka, November 2011; 2C-5O-08.
21. Kawai M. High-durability dye improves efficiency of dye-sensitized solar cells. *Nikkei Electronics* 2013; Feb.1 (http://techon.nikkeibp.co.jp/english/NEWS_EN/20130131/263532/) (Accessed October 23, 2013).
22. Mori S, Oh-oka H, Nakao H, et al. Organic photovoltaic module development with inverted device structure. *MRS Proceedings*. 2015;1737. <https://doi.org/10.1557/opl.2015.540>
23. Hosoya M, Oooka H, Nakao H, et al. Organic thin film photovoltaic modules. *Proceedings of the 93rd Annual Meeting of the Chemical Society of Japan* 2013; 21–37.
24. Zhao J, Wang A, Green MA, Ferrazza F. Novel 19.8% efficient "honeycomb" textured multicrystalline and 24.4% monocrystalline silicon solar cells. *Appl Phys Lett*. 1998;73(14):1991–1993.
25. Richter A, Benick J, Feldmann F, Fell A, Hermle M, Glunz SW. n-Type Si solar cells with passivating electron contact: identifying sources for efficiency limitations by wafer thickness and resistivity variation. *Sol Energy Mater Sol Cells*. 2017;173:96–105.
26. Haase F, Klamt C, Schäfer S, et al. Laser contact openings in dielectric layers for local poly-Si-metal contacts. *Sol Energy Mater Sol Cells*. 2018. (accepted for publication)
27. https://www.jinkosolar.com/press_detail_1380.htm (Accessed May 9, 2018).
28. Kim S, Hwang ST, Yoon W, Lee HM. High performance GaAs solar cell using heterojunction emitter and its further improvement by ELO technique. Paper 4CV.1.27, *European Photovoltaic Solar Energy Conference* 2016, Munich, June 2016.
29. Jain N, Schulte KL, Geisz JF, et al. High-efficiency inverted metamorphic 1.7/1.1eV GaInAsP/GaInAs dual junction solar cells. *Appl Phys Lett*. 2018;112(5):053905.
30. First Solar Press Release. First Solar achieves yet another cell conversion efficiency world record, 24 February 2016.
31. Wang W, Winkler MT, Gunawan O, et al. Device characteristics of CZTSSe thin-film solar cells with 12.6% efficiency. *Adv Energy Mater*. 2013;4(7). <https://doi.org/10.1002/aenm.201301465>
32. Sun K, Yan C, Liu F, et al. Beyond 9% efficient kesterite Cu₂ZnSnS₄ solar cell: fabricated by using Zn1-xCd_xS buffer layer. *Adv Energy Mater*. 2016;6(12):1600046. <https://doi.org/10.1002/aenm.201600046>
33. Jiang Q, Chu Z, Wang P, et al. Planar-structure perovskite solar cells with efficiency beyond 21%. *Adv Mater*. 2017;29(46):1703852.
34. https://en.wikipedia.org/wiki/South_China_University_of_Technology; https://en.wikipedia.org/wiki/Central_South_University
35. Chiu PT, Law DL, Woo RL, et al. 35.8% space and 38.8% terrestrial 5J direct bonded cells. *Proc. 40th IEEE Photovoltaic Specialist Conference*, Denver, June 2014; 11–13.
36. Sasaki K, Agui T, Nakaido K, Takahashi N, Onitsuka R, Takamoto T. *Proceedings, 9th International Conference on Concentrating Photovoltaics Systems*, Miyazaki, Japan 2013.
37. Essig S, Allebé C, Remo T, et al. Raising the one-sun conversion efficiency of III–V/Si solar cells to 32.8% for two junctions and 35.9% for three junctions. *Nature Energy*. 2017;2(9):17144. <https://doi.org/10.1038/nenergy.2017.144>
38. Cariou R, Benick J, Feldmann F, et al. III-V-on-silicon solar cells reaching 33% photoconversion efficiency in two-terminal configuration. *Nature Energy*. 2018;3(4):326–333. <https://doi.org/10.1038/s41560-018-0125-0>
39. Feifel M, Ohlmann J, Benick J, et al. Direct growth of III-V/silicon triple-junction solar cells with 19.7% efficiency. *IEEE J Photovoltaics*. 2018;8(6):1590–1595.
40. <https://www.oxfordpv.com/news/oxford-pv-sets-world-record-perovskite-solar-cell> (Accessed October 28, 2018).
41. Green MA, Keevers MJ, Concha Ramon B, et al. Improvements in sunlight to electricity conversion efficiency: above 40% for direct sunlight and over 30% for global. Paper 1AP.1.2, *European Photovoltaic Solar Energy Conference* 2015, Hamburg, September 2015.
42. Sai H, Matsui T, Koida T, Matsubara K. Stabilized 14.0%-efficient triple-junction thin-film silicon solar cell. *Appl Phys Lett*. 2016;109:183506. <https://doi.org/10.1063/1.49669986>
43. <http://yylab.seas.ucla.edu>
44. <http://mldevices.com/index.php/news/> (Accessed October 28, 2018).
45. Verlinden PJ, et al. Will we have >22% efficient multi-crystalline silicon solar cells? PVSEC 26, Singapore, 24–28 October, 2016.
46. Mattos LS, Scully SR, Syfu M, et al. New module efficiency record: 23.5% under 1-sun illumination using thin-film single-junction GaAs solar cells. *Proceedings of the 38th IEEE Photovoltaic Specialists Conference*, 2012.
47. Sugimoto H. High efficiency and large volume production of CIS-based modules. *40th IEEE Photovoltaic Specialists Conference*, Denver, June 2014.
48. First Solar Press Release. First Solar achieves world record 18.6% thin film module conversion efficiency, 15 June 2015.
49. Cashmore JS, Apolloni M, Braga A, et al. Improved conversion efficiencies of thin-film silicon tandem (MICROMORPH™) photovoltaic modules. *Sol Energy Mater Sol Cells*. 2016;144:84–95. <https://doi.org/10.1016/j.solmat.2015.08.022>
50. Takamoto, T. Application of InGaP/GaAs/InGaAs triple junction solar cells to space use and concentrator photovoltaic. *40th IEEE Photovoltaic Specialists Conference*, Denver, June 2014.
51. <http://www.miasole.com> (accessed 22 May, 2015).
52. Slade A, Garboushian V. 27.6% efficient silicon concentrator cell for mass production. *Technical Digest, 15th International Photovoltaic Science and Engineering Conference*, Shanghai, October 2005, 701.
53. Ward JS, Ramanathan K, Hasoon FS, et al. A 21.5% efficient Cu (In,Ga) Se₂ thin-film concentrator solar cell. *Prog Photovolt Res Appl*. 2002;10(1):41–46.
54. Dimroth F, Tibbits TND, Niemeyer M, et al. Four-junction wafer-bonded concentrator solar cells. *IEEE J Photovoltaics*. January 2016;6(1):343–349. <https://doi.org/10.1109/JPHOTOV.2015.2501729>
55. NREL Press Release NR-4514, 16 December 2014.

56. Press Release, Sharp Corporation, 31 May 2012 (accessed at <http://sharp-world.com/corporate/news/120531.html> on 5 June 2013).
57. Steiner M, Siefer G, Schmidt T, Wiesenfarth M, Dimroth F, Bett AW. 43% sunlight to electricity conversion efficiency using CPV. *IEEE Journal of Photovoltaics*. July 2016;6(4):1020-1024. <https://doi.org/10.1109/JPHOTOV.2016.2551460>
58. Green MA, Keevers MJ, Thomas I, Lasich JB, Emery K, King RR. 40% efficient sunlight to electricity conversion. *Prog Photovolt Res Appl*. 2015;23(6):685-691.
59. Chiang CJ and Richards EH. A 20% efficient photovoltaic concentrator module. *Conf. Record, 21st IEEE Photovoltaic Specialists Conference*, Kissimmee, May 1990: 861-863.
60. <http://amonix.com/pressreleases/amonix-achieves-world-record-359-module-efficiency-rating-nrel-4> (Accessed October 23, 2013).
61. van Riesen S, Neubauer M, Boos A, et al. New module design with 4-junction solar cells for high efficiencies. *Proceedings of the 11th Conference on Concentrator Photovoltaic Systems*, 2015.
62. Zhang F, Wenham SR, Green MA. Large area, concentrator buried contact solar cells. *IEEE Trans Electron Devices*. 1995;42(1):144-149.
63. Slooff LH, Bende EE, Burgers AR, et al. A luminescent solar concentrator with 7.1% power conversion efficiency. *Phys Stat Sol (RRL)*. 2008;2(6):257-259.
64. Program milestones and decision points for single junction thin films. Annual Progress Report 1984, Photovoltaics, Solar Energy Research Institute, Report DOE/CE-0128, June 1985, 7.
65. Sakata I, Tanaka Y, Koizawa K. Japan's New National R&D Program for Photovoltaics. *Photovoltaic Energy Conversion, Conference Record of the 2006 IEEE 4th world conference*, Vol 1, May 2008, 1-4.
66. Jäger-Waldau, A (Ed.). PVNET: European Roadmap for PV R&D, EUR 21087 EN, 2004.
67. Han Y, Meyer S, Dkhissi Y, et al. Degradation observations of encapsulated planar $\text{CH}_3\text{NH}_3\text{PbI}_3$ perovskite solar cells at high temperatures and humidity. *J Mater Chem A*. 2015;3(15):8139-8147.
68. Yang Y, You J. Make perovskite solar cells stable. *Nature*. 2017;544(7649):155-156.
69. Tanenbaum DM, Hermenau M, Voroshazi E, et al. The ISOS-3 interlaboratory collaboration focused on the stability of a variety of organic photovoltaic devices. *RSC Adv*. 2012;2(3):882-893.
70. Krebs FC (Ed). Stability and degradation of organic and polymer solar cells, Wiley, Chichester, 2012; Jorgensen M, Norrman K, Gevorgyan SA, Tromholt T, Andreasen B, Krebs FC. Stability of polymer solar cells. *Adv Mater*. 2012;24:580-612.
71. Krašovec UO, Bokalič M, Topič M. Ageing of DSSC studied by electroluminescence and transmission imaging. *Sol Energy Mater Sol Cells*. 2013;117:67-72.
72. Gueymard CA, Myers D, Emery K. Proposed reference irradiance spectra for solar energy systems testing. *Sol Energy*. 2002;73(6):443-467.

How to cite this article: Green MA, Hishikawa Y, Dunlop ED, et al. Solar cell efficiency tables (Version 53). *Prog Photovolt Res Appl*. 2019;27:3-12. <https://doi.org/10.1002/pip.3102>